Positron annihilation lifetime changes across the structural phase transition in nanocrystalline Fe_2O_3

S. Chakrabarti* and S. Chaudhuri†
Department of Materials Science, Indian Association for the Cultivation of Science, Jadavpur, Kolkata 700032, India

P. M. G. Nambissan‡
Nuclear and Atomic Physics Division, Saha Institute of Nuclear Physics, 1/AF Bidhannagar, Kolkata 700064, India
(Received 14 September 2004; published 22 February 2005)

Nanocrystalline samples of γ-Fe_2O_3 were prepared through chemical routes and the particles were allowed to grow by thermal treatment at different temperatures. γ-Fe_2O_3 transformed to the α phase at a temperature relatively lower than that reported for coarse-grained samples. Positron lifetimes were measured in both the phases of the samples and a significant reduction was observed across the transformation. This is attributed to the expected reduction in the unit cell volume and the nature of orientation of the nearest-neighboring atoms around the positron trapping sites. Positrons are basically annihilating from the octahedral vacancy sites in γ-Fe_2O_3 and the lifetime decreases as the nearest-neighboring atoms increasingly influence the annihilation probability of the positrons when the sample changes to the α phase. The reduction in the positron lifetime has helped to envisage the onset of the transformation earlier than that indicated by x-ray diffraction. The positron lifetimes in the intergranular region increased due to the increase in free volume associated with the atoms on the grain surfaces when the grain size reduced. Doppler broadening measurements of the annihilation γ-ray spectral line shapes were also carried out and the results supported these findings.

DOI: 10.1103/PhysRevB.71.064105 PACS number(s): 61.46.+w, 78.70.Bj, 61.10.Nz, 68.37.Lp

I. INTRODUCTION

Many properties of materials at nanometer grain sizes are structure dependent in the sense that the exact atomic arrangement in the lattice plays an important role in determining several important physical parameters like the unit cell dimensions, lattice constants, volume per atom, and radii of unoccupied lattice sites. In a number of case studies,[1–4] we have come across phase transitions that accompanied the nanocrystallization of solids. The anomalous electrical and magnetic properties of numerous nanomaterials have found their origin in the changed atomic configuration as a result of the different types of strains introduced in the materials. The studies of defects and defect-related structural alterations are important from this context and the information available from positron annihilation studies has been well appreciated in recent years.[5,6] We present in this work some interesting findings from our studies of nanocrystalline maghemite (γ-Fe_2O_3) and its transition to hematite (α-Fe_2O_3) during the coarsening of the nanometer-sized grains.

II. EXPERIMENT

For the preparation of the γ-Fe_2O_3 nanoparticles, salts of both ferrous and ferric ions were used. $FeSO_4 \cdot 7H_2O$ was the source of ferrous (Fe^{2+}) ion while the source of ferric (Fe^{3+}) ion was anhydrous $FeCl_3$. First the aqueous solution of $FeSO_4 \cdot 7H_2O$ and $FeCl_3$ was prepared with the molar ratio $FeSO_4 \cdot 7H_2O : FeCl_3 : H_2O = 1:2:1210$. NH_4OH solution (25%) was added to this solution drop by drop until the *p*H of the solution became 11. A black precipitate was produced instantly after the addition of the NH_4OH solution. This precipitate was then acidified to *p*H=3 by addition of 10.8*N* hydrochloric acid. After the acidification, the black precipitate turned into chocolate brown, indicating the formation of γ-Fe_2O_3 nanoparticles.[7,8] Finally, after stirring for 1 h, the precipitate was collected by centrifugation and dried in rotary vacuum at room temperature. The precipitate was divided into different parts and annealed at different temperatures, ranging from 300 to 1173 K, for 30 min each to obtain well-crystallized nanoparticles of different sizes. The crystallinity and the particle size of the samples were examined by x-ray diffraction and transmission electron microscope.

Positron lifetime measurements were carried out using a ^{22}Na source of approximate strength 400 kBq and a standard γ-γ coincidence setup to record the spectrum of the events due to the annihilation of positrons in the sample of interest. The source was in the form of residual deposit on a thin ($\sim$2 mg cm^{-2}) nickel foil and covered by an identical foil. It is then kept immersed in the volume of the sample (in the form of powder) taken in a glass tube. Care has been taken to ensure the annihilation of all positrons within the sample by covering the source from all sides by the powder over a thickness more than the range of positrons in it. Thus the possibility of annihilation within the walls of the glass container has been eliminated. Also the glass tube containing the sample and the source was continuously evacuated during the data acquisition to remove the air trapped in the powder.

The coincidence spectrometer used had a prompt time resolution of 240 ps (full width at half maximum) for the γ rays from a ^{60}Co source selected under the experimental conditions. With a peak to background ratio better than 4000:1, a total of about 1.5×10^6 counts were collected under each spectrum. The spectra were analyzed using RESOLUTION and POSITRONFIT.[9] We also simultaneously carried out measurements of the broadening of the spectrum of Doppler-energy-

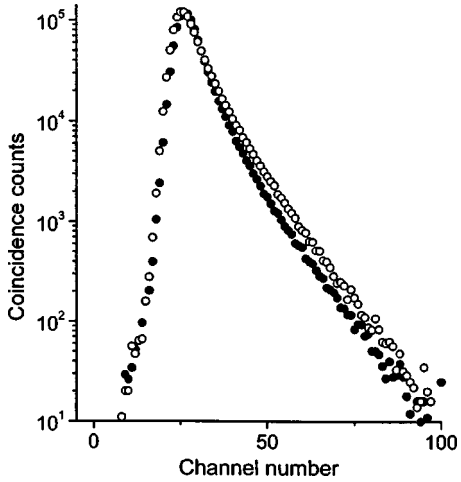

FIG. 1. Peak normalized positron lifetime spectra of the two samples of grain sizes 5 nm (γ-Fe_2O_3, open circles) and 20 nm (α-Fe_2O_3, solid circles).

shifted annihilation γ rays and estimated the line-shape parameters S and W, which are representatives of the central and wing regions corresponding to the annihilation of positrons with valence and core electrons.[10] In this case, the spectra were recorded using a high-resolution (1.28 keV full width at half maximum at 511 keV) high-purity Ge detector and an amplifier with shaping time 2 μs and until 1×10^6 counts are obtained within 511 ± 8 keV.

III. RESULTS AND DISCUSSION

The positron lifetime spectrum of each of the six samples gave three components τ_1, τ_2, and τ_3, with relative intensities I_1, I_2, and I_3, after correcting for the contribution (480 ps, 7%) from positron annihilation in the source and the nickel foil. In Fig. 1, the spectra of two samples are illustrated after normalizing the counts at the peak. To minimize the statistical uncertainties in the analysis due to the relatively fewer counts on the tail of the spectrum, the longest component τ_3 is fixed at 1.5 ns, a lifetime typical of orthopositronium atoms formed at the intergranular region. Orthopositronium atoms, with a theoretical lifetime of 140 ns, undergo faster annihilation through the pick-off process with the result that their lifetime gets reduced to a few nanoseconds.[10] The intensity I_3 of this lifetime is too small (0.3–0.6%) to have any significance in subsequent discussion. The variations of the other two lifetimes τ_1 and τ_2 and intensity $I_2(=100-I_1)$ are given in Figs. 2 and 3, respectively.

Positrons can also annihilate on the grain surfaces and the intergranular region without the formation of positronium. Owing to the diminished electron densities prevailing in such open volume defect structures, the lifetime of the positrons annihilating there is destined to be long. The intermediate-lifetime component τ_2 is a consequence of this type of annihilation and its magnitude is representative of very large vacancy clusters, equivalent to microvoids in bulk crystalline solids. In defect-free grains of nanocrystalline materials, annihilation of positrons will occur only at the grain surfaces or

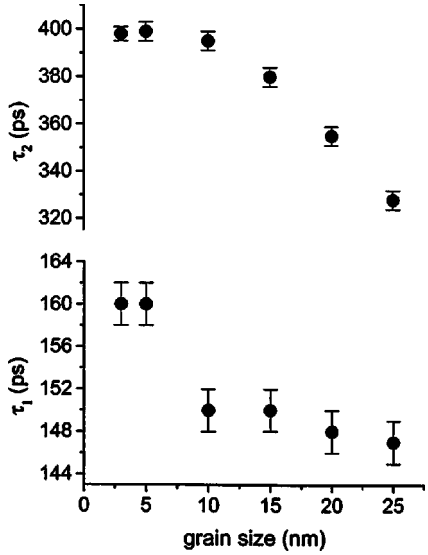

FIG. 2. Positron lifetimes τ_1 and τ_2 versus the average grain sizes of the nanocrystalline γ- and α-Fe_2O_3 samples.

intergranular regions. As the thermalized positrons diffuse over to the surface of grains whose sizes are much smaller than the thermal diffusion wavelength of positrons (~50–100 nm in typical solids[11]), the positrons will be getting trapped and annihilated within the diffused vacancies on the grain surfaces. Normally this lifetime is resolved as τ_1 and it is expected to increase steadily during the reduction in grain size owing to the increase in the net interfacial defect volume.[1,2]

The magnitudes of τ_1 obtained in the present samples are smaller than those for bulk oxides of iron (204–220 ps, derived from the bulk and defect lifetimes reported by Uhlmann *et al.*[12]). At the same time, its values in all the samples used in the present study are between that for bulk iron (110 ps) and monovacancies in it.[13] Had positron annihilation taken place at the grain surfaces as expected, a gradual reduction of its value should have been expected with increasing grain size, owing to the decrease in the excess free

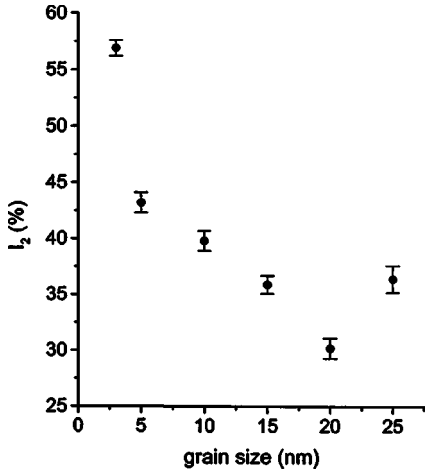

FIG. 3. The intensity I_2 versus the average grain sizes of the nanocrystalline γ- and α-Fe_2O_3 samples.

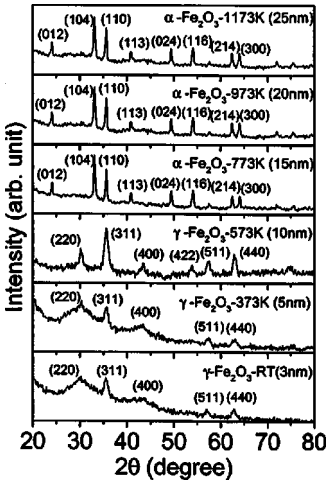

FIG. 4. X-ray diffraction patterns of the Fe_2O_3 samples, indicating the characteristic peaks of the γ and α phases.

volume associated with the atoms on the grain surfaces and hence a net decrease in the interfacial defect volume.[1,2] We note from Fig. 2 that τ_1 indeed showed a decrease but the nature of this change between the grain sizes 5 and 10 nm is not in line with the expected gradual change. The observation of such a sharp fall would rather suggest a definite transition of the structure of the crystallites and it is possible that positrons are annihilating from vacancies within the grains.

The x-ray diffraction patterns of the samples used in the present work are given in Fig. 4. The samples are identified by the temperature of heat treatment carried out for obtaining the average grain sizes indicated. From the x-ray diffraction peaks, the three samples with average grain size of 3, 5, and 10 nm can be understood as γ-Fe_2O_3 and the other three samples of higher grain sizes 15, 20, and 25 nm are in the α phase. High-resolution electron micrographs of two samples (one of the γ phase and the other of the α phase) are also shown in Figs. 5(a) and 5(b), respectively. The figures clearly reveal the presence of the respective phases with distinct lattice fringes. The lattice spacing 2.49 Å calculated from Fig. 5(a) corresponds to the (311) plane of γ-Fe_2O_3 and 2.71 Å calculated from Fig. 5(b) corresponds to the (104) plane of α-Fe_2O_3. We note that γ-Fe_2O_3 basically has the inverse spinel structure described by the formula $Fe(Fe_{5/3}\Delta_{1/3})O4$ where Δ represents the vacancies at the octahedral sites. From the values of the lattice parameters obtained from the x-ray diffraction patterns of the samples, which are given in Table I, we have estimated the radius of the octahedral vacancy site in γ-Fe_2O_3 using the relation

$$R_{oct} = (0.625 - u)a - R_0 \quad (1)$$

where a is the lattice constant, $R_0 = 1.32$ Å is the radius of the oxygen ion, and u is an oxygen ion displacement parameter whose value is 0.379 for γ-Fe_2O_3.[14] The radius of the octahedral site so obtained is 0.73 Å and it is smaller than the radius of a monovacancy in crystalline Fe($\sim$1.2 Å). Significantly enough, the lattice parameters and hence the octahedral site radii increased as the grains grew from 3 to 10 nm but, on the other hand, the positron lifetime τ_1 was reduced.

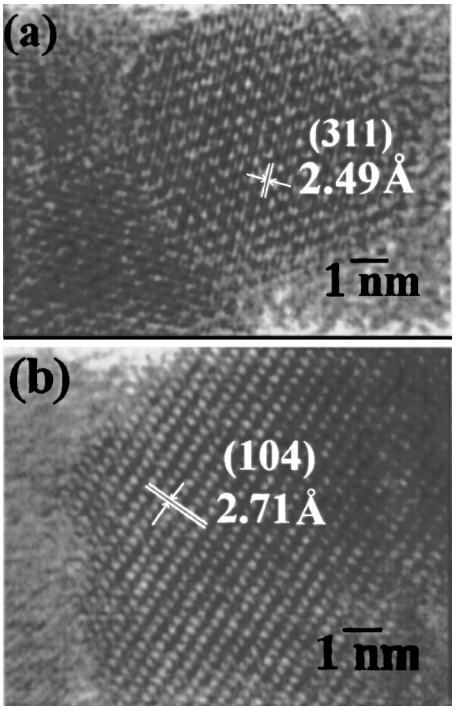

FIG. 5. High-resolution transmission electron micrographs of (a) γ-Fe_2O_3 and (b) α-Fe_2O_3, indicating the lattice fringes.

For small radii of the vacancy clusters, the positron lifetime increases with increase in their size,[15] and therefore a positron lifetime smaller than that in a monovacancy in Fe can be expected if the positrons are trapped and annihilated in the vacancies at the octahedral sites. But that the lifetime decreased contrary to the expected increase is indicative of the γ-to-α structural phase transition setting in as the temperature of heat treatment to coarsen the grains is increased (Table I).

There have been reports of size-induced phase transitions in materials like Fe_2O_3 (Ref. 16) and $PbTiO_3$,[17] and such changes have been attributed to abnormal increase in the unit cell volume that occurred as the particle size was reduced. As γ-Fe_2O_3 transforms into the α phase at grain sizes 15 nm and above, the size of the unit cell is calculated on the basis of the parameters for the rhombohedrally centered hexagonal structure.[18] The unit cell volume calculated for the samples of different grain sizes used in this study is illustrated in Fig.

TABLE I. The annealing temperatures used for obtaining nanoparticles of the average grain sizes mentioned and the lattice parameters obtained from the x-ray diffraction data analysis.

Annealing temperature (K)	Grain size (nm)	Lattice constants (Å)
300	3	$a = 8.324$
373	5	$a = 8.325$
573	10	$a = 8.344$
773	15	$a = 5.033$, $c = 13.731$
973	20	$a = 5.032$, $c = 13.732$
1173	25	$a = 5.036$, $c = 13.748$

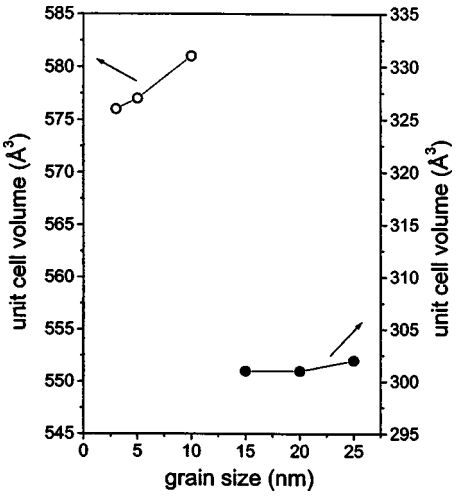

FIG. 6. The unit cell volume for the different samples of γ-Fe_2O_3 and α-Fe_2O_3 versus the average grain sizes.

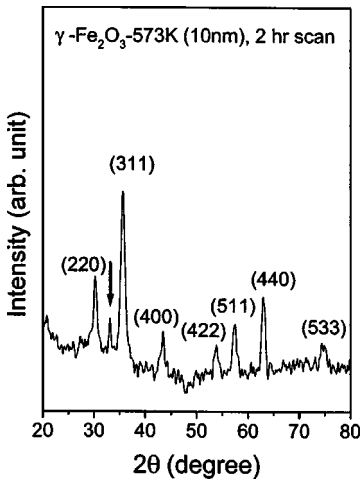

FIG. 7. X-ray diffraction pattern of the Fe_2O_3 sample of grain size 10 nm taken for longer time, resulting in the appearance of a tiny peak (shown by arrow) indicating traces of α-Fe_2O_3 in the sample otherwise considered as γ-Fe_2O_3.

6. Within the respective phases, the unit cell volume increases as the particle sizes are increased but the two phases greatly differ so far as the magnitude of the unit cell volume is concerned. The said transformation from the γ to α phase has resulted in a significant reduction in the unit cell volume (Fig. 6). Further it is noted that the Fe^{3+} ions in γ-Fe_2O_3 have neighboring O^{2-} ions with two characteristic bond lengths of 2.081 and 1.803 Å (for $a=8.325$ Å at grain size 5 nm shown in Table I) in the ratio 1:0.6.[19] In the case of α-Fe_2O_3, two sets of three Fe^{3+}-O^{2-} bonds exist with bond lengths 2.081 and 1.960 Å. As already mentioned, there exist vacancies at the octahedral sites in the γ-Fe_2O_3 phase and hence when it transforms to the α phase, the positrons trapped at these octahedral sites will feel the influence from the neighboring oxygen atoms significantly enhanced due to the unit cell contraction and this will hence result in increased probability of their eventual annihilation with electrons. As shown in Fig. 2, τ_1 has decreased by about 10 ps during this transformation and thus is in agreement with the above arguments.

There is a question about the sample of average grain size 10 nm, which the x-ray diffraction pattern in Fig. 4 has shown as in the γ phase. It was expected that the positron lifetime should have been consistent with that of the other samples of 3 and 5 nm in grain size, and should have decreased after the grain size increased above it. We find, however, that the positron lifetime τ_1 has already fallen as this grain size is reached. This gave the apprehension that possibly the transition from the γ to α phase might have already set in even before x-ray diffraction could indicate any characteristic peak. We therefore carried out a long-time scanning to seek for the appearance of any tiny peaks, which might have been hidden in the background for want of significant abundance. This proved to be the case when we observed that a small peak at $2\theta=33.17°$ had appeared in the pattern, indicating traces of the α phase present in this sample (Fig. 7). In certain experiments, the one reported for quasicrystalline $Al_{74}Mn_{20}Si_6$ for example,[20] the positron annihilation technique had been seen to sense structural changes earlier than other techniques like x-ray diffraction or calorimetric experiments could reveal such changes. The sensitivity of x-ray diffraction depends very much on the relative abundance of the phases concerned, whereas positron annihilation has versatile sensitivity for heterogeneous environments embedded in a material matrix. This has helped to envisage the possibility of occurrence of the said transformation after the grain size 5 nm, as the positron lifetime τ_1 fell drastically owing to the increased number of neighboring atoms surrounding the octahedral sites in the α phase. The cation deficiency in γ-Fe_2O_3 is partially made good by the structural rearrangement in the α phase.

It is also worth mentioning that the temperature normally observed for the γ-to-α phase transformation of Fe_2O_3 has been variably reported as 673 and 923 K.[18,21] Further, for very small particles, a higher transformation temperature was noticed with certain intermediate phases occurring in between depending on the degree of particle coarsening.[22] We observe in the present work that the transformation temperature has been significantly advanced ($\sim$573 K) as we see traces of α-Fe_2O_3 in the 10 nm sample obtained after a heat treatment at this temperature. This suggests that the driving force behind the transformation at nanometer-size particles may differ significantly from that proposed for coarse-grained samples.

The longer lifetime τ_2 is generally expected to originate from positron annihilation at the intergranular region and hence it is expected to reduce with increasing grain size (Fig. 2), as was the case with several results reported earlier.[1–3] In a true sense, the nature of variation of τ_2 should be viewed from the direction of decreasing grain size and hence its increase is reflective of a widening of the intergranular separation owing to the reduction in size of the nanocrystalline grains. Widening of the intergranular region is generally expected as a consequence of the contraction or reduction in size of the grains. The behavior of τ_2 with decreasing grain size is therefore indicative of a local enhancement in the free volume associated with the atoms on the surface of the grains. Chen *et al.*[19] have pointed out that the defects on the

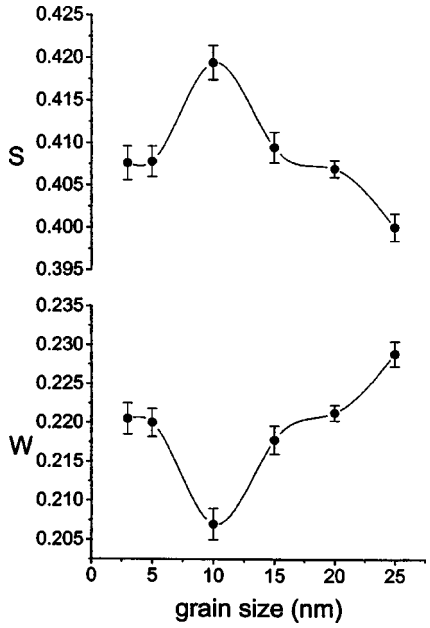

FIG. 8. The *S* and *W* parameters versus the average grain size.

surfaces of Fe_2O_3 nanoparticles are undercoordinated Fe sites with one or two O ligands missing from the structure of an octahedral coordination. This will therefore account for a relatively large value of τ_2 in the present work. Further we note that a total of eight formula units are present in one cubic unit cell of the γ phase whereas six units are present in the unit cell of the α phase.[18] The average volume per atom is estimated from the measured lattice parameters and is found to increase by about 25% as the sample transforms from the α to γ phase (in the direction of decreasing grain size). Thus the variation of τ_2 is in accordance with the results reported earlier for other nanomaterials.[1–3] The behavior of the intensity I_2 is also consistent with this interpretation since it should have increased rather monotonically with decreasing grain size due to the production of more and more interfaces (Fig. 3). Note that the difference in the values of I_2 between the γ and α phases is an appreciable 27% and is indicative of increased sensitivity of positrons to annihilate in the spinel octants in the latter due to charge imbalance created by the specific atomic distribution.[14,23]

The variation of the *S* and *W* parameters, shown in Fig. 8, further supports these arguments. Again, looking from the direction of decreasing grain size, the increase in *S* is to be interpreted as due to increase in the net open volume defects in the samples with increasing surface to volume ratio. The unexpected change between samples of grain sizes 10 and 5 nm is again indicative of positrons annihilating in two different samples of differing electronic structure and is thus consistent with the phase transition occurring at this stage. *W* varies in the reverse order as is expected. Notwithstanding these indications, the mean positron lifetime τ_m defined as

$$\tau_m = (\tau_1 I_1 + \tau_2 I_2 + \tau_3 I_3)/(I_1 + I_2 + I_3) \quad (2)$$

increases monotonically with decreasing grain size (Fig. 9), indicating the presence of more and more open volume defects at the larger number of interfaces in samples composed of smaller grains, as is to be expected.

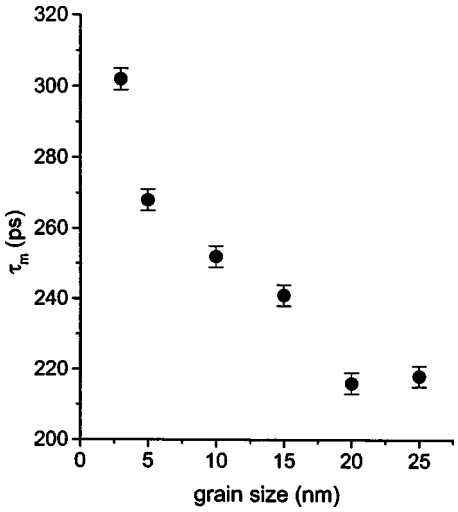

FIG. 9. The mean positron lifetime τ_m versus the average grain size.

IV. CONCLUSIONS

A characteristic change in positron lifetimes across the structural transformation from the γ to the α phase of nanocrystalline Fe_2O_3 has been found, in accordance with the reduction in the unit cell volume and the nature of orientation of the nearest-neighboring atoms around the positron trapping sites. It is worth noting that the temperature necessary for the transformation has been advanced due to the nanocrystalline composition of the samples and the reduction in the positron lifetime has helped to envisage the onset of the transformation earlier than indicated by x-ray diffraction. Further, the increase of the positron lifetimes in the intergranular region when the grain size is reduced can be attributed to the increase in free volume associated with the atoms on the grain surfaces. The results from Doppler broadening measurements of the annihilation γ-ray spectral line shapes also supported these findings.

ACKNOWLEDGMENT

The authors are grateful to Subhajit Biswas for his help during the experiments.

*Email address: mssc3@mahendra.iacs.res.in
†Email address: mssc2@mahendra.iacs.res.in
‡Corresponding author. Email address: gopal@anp.saha.ernet.in

[1] M. Mukherjee, D. Chakravorty, and P. M. G. Nambissan, Phys. Rev. B **57**, 848 (1998).
[2] P. P. Chattopadhyay, P. M. G. Nambissan, S. K. Pabi, and I. Manna, Phys. Rev. B **63**, 054107 (2001).
[3] P. M. G. Nambissan, C. Upadhyay, and H. C. Verma, J. Appl. Phys. **93**, 6320 (2003).
[4] I. Manna, P. P. Chattopadhyay, P. Nandi, and P. M. G. Nambissan, Phys. Lett. A **328**, 246 (2004).
[5] H.-E. Schaefer, R. Wurschum, R. Birringer, and H. Gleiter, Phys. Rev. B **38**, 9545 (1988).
[6] H.-E. Schaefer and R. Wurschum, Phys. Lett. A **119**, 370 (1987).
[7] S. Chakrabarti, S. K. Mandal, B. K. Nath, D. Das, D. Ganguli, and S. Chaudhuri, Eur. Phys. J. B **34**, 163 (2003).
[8] N. J. Cherepy, D. B. Liston, J. A. Lovejoy, H. Deng, and J. Z. Zheng, J. Phys. Chem. B **102**, 770 (1998).
[9] P. Kirkegaard, M. Eldrup, O. E. Mogensen, and N. J. Pedersen, Comput. Phys. Commun. **23**, 307 (1981).
[10] P. Asoka-Kumar, K. G. Lynn, and D. O. Welch, J. Appl. Phys. **76**, 4935 (1994).
[11] B. Bergersen, E. Pajanne, P. Kubica, M. J. Stott, and C. H. Hodges, Solid State Commun. **15**, 1377 (1974).
[12] K. Uhlmann, D. T. Britton, and S. Heger, Mater. Sci. Forum **175-178**, 225 (1995).
[13] P. Hautojarvi, T. Judin, A. Vehanen, J. Yli-Kaupilla, J. Johansson, J. Verdone, and P. Moser, Solid State Commun. **29**, 855 (1979).
[14] J. Smit and H. P. J. Wijn, *Ferrites—Physical Properties of Ferromagnetic Oxides in Relation to Their Technical Applications* (N. V. Philips Gloeilampenfabrieken, Eindhoven, Holland, 1959).
[15] M. J. Puska and R. M. Nieminen, J. Phys. F: Met. Phys. **13**, 333 (1983).
[16] Pushan Ayyub, Manu Multani, Mustansir Barma, V. R. Palkar, and R. Vijayaraghavan, J. Phys. C **21**, 2229 (1988).
[17] Soma Chattopadhyay, Pushan Ayyub, V. R. Palkar, and Manu Multani, Phys. Rev. B **52**, 13 177 (1995).
[18] Radek Zboril, Miroslav Mashlan, and Dimitris Petridis, Chem. Mater. **14**, 969 (2002).
[19] Lin X. Chen, Tao Liu, Marion C. Thurnauer, Roseann Csencsits, and Tijana Rajh, J. Phys. Chem. B **106**, 8539 (2002).
[20] R. Chidambaram, M. K. Sanyal, P. M.G. Nambissan, and P. Sen, J. Phys.: Condens. Matter **2**, 251 (1990).
[21] G. Ennas, A. Musinu, G. Piccaluga, D. Zedda, D. Gatteschi, C. Sangregorio, J. L. Stanger, G. Concas, and G. Spano, Chem. Mater. **10**, 495 (1998).
[22] E. Tronc, C. Chaneac, and J. P. Jolivet, Solid State Chem. **139**, 93 (1998).
[23] F. Scordari, in *Fundamentals of Crystallography*, edited by C. Giacovazzo (Oxford University Press, New York, 1992).